

Manuscript Number:

Title: Site selective spectroscopy in BaYF<sub>5</sub>:RE<sub>3+</sub> (RE = Eu, Sm) nano-glass-ceramics

Article Type: Full Length Article

Keywords: BaYF<sub>5</sub> nanocrystals, rare-earth ions, sol-gel method, glass-ceramics, luminescence.

Corresponding Author: Dr. Javier del-Castillo,

Corresponding Author's Institution:

First Author: Javier del-Castillo

Order of Authors: Javier del-Castillo; A. C. Yanes; S. Abé; P. F. Smet

Abstract: Trivalent rare-earth (RE = Eu, Sm) doped transparent nano-glass-ceramics comprising BaYF<sub>5</sub> nanocrystals were successfully obtained by appropriate heat-treatment of the corresponding precursor sol-gel glasses. Their structural and spectroscopic properties were investigated and compared with those for Eu<sup>3+</sup>-doped-BaYF<sub>5</sub> nanocrystals prepared by a solvothermal method. X-ray Diffraction, Transmission Electron Microscopy and Energy Dispersive X-ray Spectroscopy measurements confirmed the distribution of BaYF<sub>5</sub> nanocrystals in the glass matrix, presenting a cubic phase structure with space group Fm-3m. In order to achieve a further structural characterization, the luminescence properties of the Eu<sup>3+</sup> and Sm<sup>3+</sup> dopants were also used as sensitive probes. The reduction in the emission intensities of hypersensitive transitions 5D<sub>0</sub>->7F<sub>2</sub> and 4G<sub>5/2</sub>->6H<sub>9/2</sub> for Eu<sup>3+</sup> and Sm<sup>3+</sup> ions respectively, along with time-resolved measurements, confirm the distribution of a significant fraction of RE ions into the fluoride nanocrystal environment. These results suggest that BaYF<sub>5</sub> nano-glass-ceramics doped with Eu<sup>3+</sup> or Sm<sup>3+</sup> can be considered as potential red-emitting phosphors for the development of white LEDs under near UV excitation.

Dear Editor:

Hereby we submit a manuscript entitled “**Site selective spectroscopy in BaYF<sub>5</sub>:RE<sup>3+</sup> (RE = Eu, Sm) nano-glass-ceramics**” by *J. del-Castillo, A.C. Yanes, S. Abé and P. F. Smet* for publication in **Journal of Alloys and Compounds**. The manuscript reports on transparent nano-glass-ceramics containing Ln<sup>3+</sup>-doped **BaYF<sub>5</sub>** nanocrystals embedded in amorphous silica matrix, successfully obtained by heat treatment of precursor sol-gel glasses, for the first time, focussing the attention on the structure properties of cubic BaYF<sub>5</sub> nanocrystal. Moreover, Eu<sup>3+</sup> doped-BaYF<sub>5</sub> NCs were successfully obtained by a solvothermal method in order to compare and confirm the cubic structure of fluoride NCs in the nGCs system. We believe this paper will be of interest for wide audience of your journal.

On behalf of co-authors

J. del-Castillo

*University of La Laguna, Tenerife, Spain*

*La Laguna, 17<sup>th</sup> December, 2014*

## **Prime Novelty Statement**

To,

The Editor-in-chief,

Journal of Alloys and Compounds

In the submitted manuscript, I am reporting, for the first time, the synthesis of sol-gel transparent glass-ceramics comprising  $\text{Eu}^{3+}$  or  $\text{Sm}^{3+}$ -doped cubic  $\text{BaYF}_5$  nanocrystals. I am also reporting the preparation of  $\text{Eu}^{3+}$ -doped  $\text{BaYF}_5$  nanocrystals by solvothermal method, and the study of their luminescent properties to compare with the  $\text{Eu}^{3+}$ -doped nGCs, Further, I have used  $\text{Eu}^{3+}$  and  $\text{Sm}^{3+}$  as probe ions in the glass-ceramics, to distinguish between amorphous and like-crystalline environments, confirming the incorporation of a large fraction of RE ions into the  $\text{BaYF}_5$  nanocrystals. These results suggest that  $\text{BaYF}_5$  glass-ceramics doped with  $\text{Eu}^{3+}$  or  $\text{Sm}^{3+}$  can be considered as potential red-emitting phosphors for the development of white LEDs under near UV excitation. In view to this, the publication of this work in Journal of Alloys and Compounds will be valuable.

Sincerely yours,

Dr. J. del-Castillo  
Dpto de Física,  
University of La Laguna,  
Spain

## Site selective spectroscopy in BaYF<sub>5</sub>:RE<sup>3+</sup> (RE = Eu, Sm) nano-glass-ceramics

J. del-Castillo<sup>1\*</sup>, A.C. Yanes<sup>1</sup>, S. Abé<sup>2,3</sup>, P. F. Smet<sup>2,3</sup>

<sup>1</sup> Dpto. Física, Universidad de La Laguna, 38206 La Laguna, Tenerife, Spain

<sup>2</sup> LumiLab, Department of Solid State Sciences, Ghent University, Krijgslaan 281-S1, 9000 Gent, Belgium

<sup>3</sup> Center for Nano- and Biophotonics (NB Photonics), Ghent University, Belgium.

### Abstract

Trivalent rare-earth (RE = Eu, Sm) doped transparent nano-glass-ceramics comprising BaYF<sub>5</sub> nanocrystals were successfully obtained by appropriate heat-treatment of the corresponding precursor sol-gel glasses. Their structural and spectroscopic properties were investigated and compared with those for Eu<sup>3+</sup>-doped-BaYF<sub>5</sub> nanocrystals prepared by a solvothermal method. X-ray Diffraction, Transmission Electron Microscopy and Energy Dispersive X-ray Spectroscopy measurements confirmed the distribution of BaYF<sub>5</sub> nanocrystals in the glass matrix, presenting a cubic phase structure with space group *Fm-3m*. In order to achieve a further structural characterization, the luminescence properties of the Eu<sup>3+</sup> and Sm<sup>3+</sup> dopants were also used as sensitive probes. The reduction in the emission intensities of hypersensitive transitions <sup>5</sup>D<sub>0</sub>→<sup>7</sup>F<sub>2</sub> and <sup>4</sup>G<sub>5/2</sub>→<sup>6</sup>H<sub>9/2</sub> for Eu<sup>3+</sup> and Sm<sup>3+</sup> ions respectively, along with time-resolved measurements, confirm the distribution of a significant fraction of RE ions into the fluoride nanocrystal environment. These results suggest that BaYF<sub>5</sub> nano-glass-ceramics doped with Eu<sup>3+</sup> or Sm<sup>3+</sup> can be considered as potential red-emitting phosphors for the development of white LEDs under near UV excitation.

Keywords: BaYF<sub>5</sub> nanocrystals, rare-earth ions, sol-gel method, glass-ceramics, luminescence.

Corresponding author: fjvargas@ull.edu.es

## Introduction

The interest in rare-earth (RE) doped low-phonon energy nano-materials has grown in recent decades due to their promising applications in light-emitting devices, biological labelling and imaging, up-conversion (UC) lasers, high density memories, among others [1-2]. In particular, RE doped oxyfluoride nano-glass-ceramics (nGCs) have attracted attention due to the mechanical and chemical properties of oxide glasses [3] and the lower phonon energies encountered in fluorides, which means that non-radiative quenching of emission is limited and therefore higher efficiencies can be reached. Thus, the nGCs present a high degree of transparency, due to the small nanocrystals (NCs) being dispersed in a transparent matrix (e.g. silica). In addition, energy transfer (ET) processes between neighbouring RE ions are favoured for the shortening of their interionic distances in the precipitated NCs. In this sense, the distribution of the optically active RE ions into the fluoride environment is of particular interest in view of the luminescent properties.

There is a large collection of reported work on fluorides such as  $AREF_4$ ,  $MF_2$ ,  $REF_3$  and  $xMF_2-yREF_3$  (A=alkali metal ions, M being a group-II element) [4-14].  $MF_2-REF_3$  systems have been extensively investigated and used as good host matrix for many optically active ions, with application in laser crystals and as UC material [15]. In this sense,  $BaYF_5$  is an interesting host material due to its structure and optical properties [16-18], being transparent in a large electromagnetic domain and with a low maximum phonon frequency, leading to a potentially large number of emitting levels. Although there is an extensive literature on RE doped- $BaYF_5$  NCs [16-19], only a few about nGCs comprising  $BaYF_5$  NCs were reported [20-23]. These  $BaYF_5$  nGCs can be obtained from low cost and non-poisonous  $BaF_2$ ,  $YF_3$  and  $Y_2O_3$  raw materials using the conventional thermal quenching method [24], however the volatilization at high melting temperature is problematic. An improvement in the nGCs preparation is achieved by using the sol-gel technique, allowing the formation of the precursor glasses at room temperature, and their corresponding nGCs at comparatively lower temperatures. Thus, by avoiding the evaporation losses, it is possible to precisely control the nGCs' chemical composition [25]. Moreover, the RE ions can be introduced into the "sol" giving rise to an excellent homogeneity in the final material, in contrast to common diffusion driven solid state reactions.

Within the large set of RE ions, the red emission of  $\text{Eu}^{3+}$  was essential in the development of (compact) fluorescent lights and cathode ray tubes, as it offers a great return in luminous efficacy, due to the narrow-banded emission in the red part of the visible spectrum where the eye sensitivity is still relatively high. However,  $\text{Eu}^{3+}$  ions are in principle not a good choice for use in LED conversion phosphors, due to the low absorption strength of the 4f-4f transitions in  $\text{Eu}^{3+}$  in the near-UV to blue region. To obtain sufficiently high absorption strength, there are basically two options. First, a  $\text{Eu}^{3+}$  based phosphor can be processed into a dense, pore-free ceramic disk, in which the absorption can be enhanced, while keeping scattering losses low [26]. However, it is often not straightforward or cost-effective to convert common powder phosphors into high density ceramic platelets. The second option is pursued in this work, where a  $\text{Eu}^{3+}$  containing luminescent NC is naturally embedded in a transparent matrix. In this way, scattering due to a mismatch of the refractive index is avoided when the NCs are sufficiently small.

In this work we present for the first time, as far as we know, sol-gel derived nGCs containing  $\text{Eu}^{3+}$  or  $\text{Sm}^{3+}$  doped- $\text{BaYF}_5$  NCs. A complete structural analysis has been carried out, leading to the assignment of the  $\text{BaYF}_5$  crystalline phase as cubic. In literature at least two different assignments can be found, related to tetragonal and cubic phases of  $\text{BaYF}_5$  [27 and refs therein]. A major issue for NCs embedded in nGCs is the incorporation of the dopant ions. For this, the local environment of RE ions can be analysed taking into account their luminescent features. In some cases transition probabilities are especially sensitive to the local symmetry, and therefore can be used as probe ions. In the case of  $\text{Eu}^{3+}$  and  $\text{Sm}^{3+}$  ions, the electric dipole (ED) character of hypersensitive transitions  $^5\text{D}_0 \rightarrow ^7\text{F}_2$  and  $^4\text{G}_{5/2} \rightarrow ^6\text{H}_{9/2}$  respectively, presents high sensitivity to the local environment [28]. Thus, by using  $\text{Eu}^{3+}$  and  $\text{Sm}^{3+}$  it is possible to discern between crystalline and glassy environments by means of site-selective spectroscopy and time-resolved measurements, especially if the crystalline host contains centrosymmetric sites. Moreover,  $\text{Eu}^{3+}$  doped- $\text{BaYF}_5$  NCs were successfully obtained by a solvothermal method in order to compare and confirm the cubic structure of fluoride NCs in the nGCs system.

## **Experimental**

Silica glasses with a composition consisting of 95SiO<sub>2</sub>-5BaYF<sub>5</sub> doped with 0.1 of Eu<sup>3+</sup> or Sm<sup>3+</sup> ions (in mol%) were obtained by sol-gel method in a similar way as described in ref. [29]. Tetraethoxysilane (TEOS) Si(OCH<sub>2</sub>CH<sub>3</sub>)<sub>4</sub>, used as a source of SiO<sub>2</sub>, was hydrolysed for 1 h at room temperature with a mixed solution of ethanol and deionized H<sub>2</sub>O, using acetic acid as a catalyst. The molar ratio of TEOS:ethanol:H<sub>2</sub>O:CH<sub>3</sub>COOH was 1:4:10:0.5. As sources of Ba and Y, Ba(CH<sub>3</sub>COO)<sub>3</sub> · xH<sub>2</sub>O and Y(CH<sub>3</sub>COO)<sub>3</sub> · xH<sub>2</sub>O were used. The required quantities of Ba(CH<sub>3</sub>COO)<sub>3</sub> · xH<sub>2</sub>O, Y(CH<sub>3</sub>COO)<sub>3</sub> · xH<sub>2</sub>O, Eu(CH<sub>3</sub>COO)<sub>3</sub> · xH<sub>2</sub>O and Sm(CH<sub>3</sub>COO)<sub>3</sub> · xH<sub>2</sub>O were dissolved in a CF<sub>3</sub>COOH and H<sub>2</sub>O solution, which were slowly mixed with the initial solution. The molar ratio of metal ions to CF<sub>3</sub>COOH was 1:5. In order to make the solution homogeneous, it was stirred vigorously for 1 h at room temperature. A highly transparent gel was obtained by leaving the resultant homogeneous solution in a sealed container at 35 °C for several days. The gels were then dried by slow evaporation for approximately four weeks to remove residual water and solvents. Finally, these sol-gel glasses were heat-treated in an air atmosphere at 750 °C in order to achieve the controlled precipitation of BaYF<sub>5</sub> nanocrystals, required to produce transparent nGCs.

Moreover, BaYF<sub>5</sub> NCs doped with 2% of Eu<sup>3+</sup> ions were prepared through a solvothermal method using oleic acid as capping ligand to control the particle growth and prevent the NCs from aggregation, as described in refs [2,27]. In brief, 2 ml deionized H<sub>2</sub>O, 0.6 g NaOH, 10 ml ethanol and 20 ml oleic acid were mixed together under vigorous stirring to form a transparent homogeneous solution. Then, an aqueous solution (4 ml) of Ba(NO<sub>3</sub>)<sub>2</sub> (0.5 mmol) and a stoichiometric amount of Y(NO<sub>3</sub>)<sub>3</sub>, Eu(NO<sub>3</sub>)<sub>3</sub> were added to above solution. After that, 1 ml of aqueous solution containing 2.5 mmol NH<sub>4</sub>F was added. After stirring for another 20 min, the as-obtained homogeneous colloidal solution was transferred into a 50 ml stainless Teflon-lined autoclave and kept at 200 °C for 24 h. The autoclave was naturally cooled down to room temperature. The precipitate deposited at the bottom of Teflon vessel was collected by centrifugation, washed with ethanol and deionized water several times, and then dried in air at 60 °C for 24 h. The obtained NCs were dispersed in toluene (2% wt) for all spectroscopic measurements.

Powder X-ray diffraction (XRD) patterns of the samples were recorded with a Philips X'Pert Pro diffractometer equipped with a primary monochromator, a Cu K<sub>α1α2</sub> radiation source, and an X'Celerator detector. The XRD patterns were collected with a

step of  $0.016^\circ$  in the  $2\theta$  angular range from  $15$  to  $85^\circ$  and an acquisition time of  $2$  h. Furthermore, the diffraction pattern of  $\text{LaB}_6$  was used as an internal standard to calibrate the parameters of the instrument profile. Transmission electron microscopy (TEM-HRTEM) images were obtained using a JEOL 2200FS microscope operating at  $200$  kV, equipped with a Field Emission Gun, which allowed us to achieve a point-to-point resolution of  $0.17$  nm. Samples were prepared by dispersing fine powder, obtained by grinding the samples, in ethanol and dropping them onto carbon-coated copper grids. Selected areas of the HRTEM images were mathematically filtered by means of Fast Fourier Transform (FFT) analysis resulting in Power Spectra patterns, corresponding to the eigen-frequencies of the observed NCs. Further, the relevant frequencies were selected to filter the noise in the zoomed areas of the HRTEM images and to produce higher contrast images of the atomic planes of the observed NCs.

Luminescence measurements were performed using an Edinburgh Instruments' FLS920 fluorescence spectrometer, with a  $0.3$  m double excitation monochromator and an  $0.3$  m emission monochromator, to record the emission spectra in the wavelength range of  $200$ - $850$  nm (with a Hamamatsu R928 photomultiplier tube). The time resolved photoluminescence measurements were carried out using a PTI spectrometer, where a  $75$ W Xenon flash lamp acts as excitation source. All spectra were collected at room temperature and corrected for the instrumental response.

## Results and Discussion

The structural characterization was carried out by means of XRD patterns and TEM and HRTEM images. Fig. 1(a) presents the XRD pattern of  $\text{BaYF}_5$  nGCs doped with  $0.1$   $\text{Eu}^{3+}$  (mol%), showing a broadband characteristic of the  $\text{SiO}_2$  along with diffraction peaks at  $26.3$ ,  $30.4$ ,  $43.5$ ,  $51.5$ ,  $53.9$ ,  $63.2$ ,  $69.7$ ,  $71.8$  and  $79.8^\circ$  in  $2\theta$  range from  $15$  to  $85^\circ$ . By using the strongest peak at  $2\theta=26.3^\circ$  and the Scherrer equation, a mean NCs size of  $11$  nm was obtained. This value is in a reasonably good agreement with the size observed by TEM imaging, Fig. 1(b), where the NCs are visible as dark spots, dispersed in the amorphous silica network of the nGC system. Moreover, they are appreciably smaller than those obtained previously in  $\text{BaYF}_5$  nGCs by K. Biswas et al.

[20] around 30-50 nm, S. Huang et al. [21] and M. Gu et al. [22] around 11-31 nm and F. Liu et al. [23] around 25 nm.

In order to confirm the presence of BaYF<sub>5</sub> NCs in the nGC system, Eu<sup>3+</sup>-doped BaYF<sub>5</sub> NCs were prepared by solvothermal method. By using Energy Dispersive X-ray Spectroscopy (EDX) analysis in the as-prepared material, see Fig. 2(a), it is possible to determine its real composition. Peaks corresponding to Ba, Y and F are observed along with Cu and C peaks originating from the copper grid. The atomic ratios of Ba/Y/F are 1/1.05/4.89, which is in excellent agreement with the theoretical atomic Ba/Y/F ratio of 1/1/5 in BaYF<sub>5</sub> taking the accuracy of EDX spectroscopy into account.

Corresponding XRD pattern of Eu<sup>3+</sup>-doped BaYF<sub>5</sub> NCs is also included in Fig. 1(a). All XRD peaks, in BaYF<sub>5</sub> nGCs and also in the BaYF<sub>5</sub> NCs, can be assigned to the cubic structure of BaYF<sub>5</sub> [16] similar to the standard peaks of BaCeF<sub>5</sub> (JCPDS 43-0394, space group *Fm-3m*), also shown in Fig. 1(a) for comparison. There is a slight shift in all XRD peaks to higher 2 $\theta$  side, due to the possible variation of the cell parameter related to the radius of Y<sup>3+</sup> ions [8]. Thus, taking initially the structure of BaCeF<sub>5</sub> in a Rietveld refinement, we can estimate the lattice constant value of  $a = 5.853$  and  $5.879$  Å, for BaYF<sub>5</sub> nGCs and NCs, respectively, in a good agreement with previous results [16, 27].

Next, to complete the structural characterization, HRTEM images were collected for the Eu<sup>3+</sup>-doped BaYF<sub>5</sub> NCs. The observed NCs in the HRTEM bright-field micrograph are clearly distinguished as dark particles, see Fig. 2(b), with mean size around 20-30 nm. This is comparable with the size estimated by the Scherrer equation (around 30 nm). The power spectrum from the squared NCs lead us to obtain filtered images by using the frequencies determined from the FFT pattern, see insets in Fig. 2(b). The interplanar distances of 3.34 and 2.88 Å correspond to (111) and (200) planes of BaYF<sub>5</sub> cubic phase respectively. The results from HRTEM analysis are consistent with the previously analysed XRD data.

Most trivalent RE ions show visible or infrared emissions, due to electron transitions within the 4f<sup>n</sup> electronic configurations. Because the 4f electrons are well shielded from the crystal environment, the emission and excitation peaks are relatively narrow. Besides the use of lanthanide ions for luminescence based applications, the dependency of the relative intensity of certain transitions, as well as their lifetime and multiplet splitting, can be used as a probe for the local environment of the RE ions.

The luminescent features of  $\text{Eu}^{3+}$  and  $\text{Sm}^{3+}$  ions could therefore reveal whether the RE ions are actually incorporated in the NCs or distributed in the nGCs, outside the NCs. Fig. 3(a and b) shows excitation and emission spectra of the  $\text{BaYF}_5$  nGCs doped with 0.1 $\text{Eu}^{3+}$  (mol%), detecting and exciting at the indicated wavelengths. For the excitation, spectra have been normalized at the maximum of the intensity at 525 nm ( ${}^7\text{F}_0 \rightarrow {}^5\text{D}_1$ ), because this transition is weakly dependent on the local environment of the  $\text{Eu}^{3+}$  ions. These spectra present mainly excitation peaks of  $\text{Eu}^{3+}$  ions corresponding to transitions from  ${}^7\text{F}_0$  ground level to the excited levels labelled in the figure, according the energy level diagram included in the inset of Fig. 3(a). In particular, the  ${}^7\text{F}_0 \rightarrow {}^5\text{D}_2$  transition (around 464 nm) shows electric dipole character (ED), hypersensitive to the local structure around  $\text{Eu}^{3+}$  ions, and therefore forbidden in the centrosymmetric environments. Thus, by detecting the emission  ${}^5\text{D}_0 \rightarrow {}^7\text{F}_1$  at 590 nm (with magnetic dipole character MD) or the  ${}^5\text{D}_0 \rightarrow {}^7\text{F}_2$  at 616 nm (with electric dipole character ED), insensitive and hypersensitive to the crystal field environment for the  $\text{Eu}^{3+}$  ions respectively, significant differences can be observed. The intensity of the excitation peak corresponding to the transition  ${}^7\text{F}_0 \rightarrow {}^5\text{D}_2$  at 464 nm, is diminished when detecting at 590 nm instead of 616 nm. This result along with a better resolved Stark structure of the excitation bands below 380 nm can be related with a more crystalline environment for the  $\text{Eu}^{3+}$  ions.

On the other hand, the emission spectra upon excitation at 394 and 464 nm have been normalized at the maximum of the ( ${}^5\text{D}_0 \rightarrow {}^7\text{F}_1$ ) transition at 590 nm, with MD character, which is non-sensitive to local site symmetry, see Fig. 3(b). Upon excitation at around 394 nm, emissions originating from the  ${}^5\text{D}_2$ ,  ${}^5\text{D}_1$  and  ${}^5\text{D}_0$  levels are observed, which can be related with a low-phonon-energy environment for  $\text{Eu}^{3+}$  ions. However, by exciting at 464 nm (i.e. promoting the excitation of  $\text{Eu}^{3+}$  ions with low symmetry), the relative intensity of all emissions reduces and, in particular the emissions coming from upper-lying  ${}^5\text{D}_2$  and  ${}^5\text{D}_1$  levels almost disappear, related with glassy environments that present higher phonon energy. To clarify this assumption, we used the asymmetry ratio R defined as the ratio between the ED  ${}^5\text{D}_0 \rightarrow {}^7\text{F}_2$  to MD  ${}^5\text{D}_0 \rightarrow {}^7\text{F}_1$  transitions. This ratio can be useful as a measurement of how close the local environment is to centrosymmetric [28,30]. In this case, R value of 0.8 was obtained when exciting at 394 nm which confirms that the environment of  $\text{Eu}^{3+}$  ions gets closer to a centrosymmetric site, related with their distribution into the  $\text{BaYF}_5$  NCs. On the contrary, exciting at 464

nm, R value of 3.5 is obtained, associated with a non-centrosymmetric environment for  $\text{Eu}^{3+}$  ions that remain in the silica glassy phase.

Next, we analyse the excitation and emission spectra of  $\text{Eu}^{3+}$  doped- $\text{BaYF}_5$  NCs, where similar luminescent features should be expected. Thus, the excitation spectrum, see Fig. 3(c), shows well-resolved excitation peaks of  $\text{Eu}^{3+}$  ions, similar to the peaks previously observed in the  $\text{BaYF}_5$  nGCs detecting at 590 nm. It should be noticed that the intensity of the  ${}^7\text{F}_0 \rightarrow {}^5\text{D}_2$  excitation peak at 464 nm also diminishes when comparing with the excitation spectrum of the  $\text{BaYF}_5$  nGCs detecting at 616 nm (glassy environment). The corresponding emission spectrum, see Fig. 3(d), shows, besides the characteristic emissions from the  ${}^5\text{D}_0$  level, emission peaks from the  ${}^5\text{D}_2$  and  ${}^5\text{D}_1$  levels, which are more significant than those observed in the nGCs system when exciting at the same wavelength, which is related with a lower-phonon energy environment for the  $\text{Eu}^{3+}$  ions. The lower R value of 0.4 for  $\text{Eu}^{3+}$  doped- $\text{BaYF}_5$  NCs when comparing with the corresponding one in the nGCs, (R value = 0.8) can be explained by the higher symmetry environment for the  $\text{Eu}^{3+}$  ions. These results are in good agreement with a larger NC size as it was observed by XRD and HRTEM measurements.

Furthermore, to confirm the previously observed differences between crystalline and glassy environments for  $\text{Eu}^{3+}$  ions in the  $\text{BaYF}_5$  nGCs, time-resolved photoluminescence measurements were carried out in the nGCs system and in the NCs. In this sense, the behaviour of the luminescence decay from the  ${}^5\text{D}_0$  level was measured, selecting the excitation and detection wavelengths corresponding to the different sites previously observed. Fig. 4 shows time-resolved photoluminescence decays for  $\text{BaYF}_5$  nGCs, exciting at 464 nm and detecting the 616 nm emission (corresponding to a glassy environment), and exciting at 394 nm and detecting the 590 nm emission (corresponding to a close to inversion symmetry site associated to nanocrystalline  $\text{BaYF}_5$  environment). In the first case, an effective lifetime value of 1.63 ms related to the amorphous environment of  $\text{Eu}^{3+}$  ions in the glass phase is obtained from the area under the curve through the expression  $\tau_{eff} = \int_0^\infty I(t)dt/I(0)$ , see Table.1. However in the second case, a value of 9.88 ms that can be related with  $\text{Eu}^{3+}$  ions distributed inside the  $\text{BaYF}_5$  NCs, is obtained. To confirm this assumption, a value of 9.12 ms, similar to the previous one obtained in the nGCs, was obtained in the  $\text{Eu}^{3+}$ -doped  $\text{BaYF}_5$  NCs, exciting at 394 nm and detecting at 590 nm.

Finally, in order to complete the structural analysis we also study the luminescence features of the  $\text{Sm}^{3+}$ -doped  $\text{BaYF}_5$  nGCs. In a similar way than  $\text{Eu}^{3+}$  ions,  $\text{Sm}^{3+}$  ions can also act as a spectroscopic probe of the local structure around RE ions. This is related with the ED character of the  ${}^4\text{G}_{5/2} \rightarrow {}^6\text{H}_{9/2}$  hypersensitive transition, for which the intensity increases as the symmetry of the local environment of the luminescent site decreases [31]. The excitation spectrum of the  $\text{Sm}^{3+}$ -doped  $\text{BaYF}_5$  nGCs, obtained by detecting the 596 nm emission, corresponding to the  ${}^4\text{G}_{5/2} \rightarrow {}^6\text{H}_{7/2}$  transition, presents peaks arising from the ground state  ${}^6\text{H}_{5/2}$  to excited levels labelled in the Fig. 5(a) according to its energy level diagram. The corresponding emission spectrum upon excitation at the most intense excitation peak, at 399 nm, is presented in Fig. 5(b) showing four main emissions in the yellow-to-red part of the visible spectrum coming from the  ${}^4\text{G}_{5/2}$  level. On the other hand in  $\text{SiO}_2\text{-SnO}_2$  nGCs doped with  $\text{Sm}^{3+}$  ions, previously studied by authors [32], the relative intensities of these emission peaks are markedly different when  $\text{Sm}^{3+}$  ions remain in silica glassy environment, see Fig. 5(b). Similar to the case of  $\text{Eu}^{3+}$  ions, the intensity ratio R between the  ${}^4\text{G}_{5/2} \rightarrow {}^6\text{H}_{9/2}$  (ED character, hypersensitive to the local environment) to  ${}^4\text{G}_{5/2} \rightarrow {}^6\text{H}_{5/2}$  (predominant MD character, insensitive to the local environment) emission transitions for  $\text{Sm}^{3+}$  was calculated. The R values of 1.4 and 3.7 were obtained for the  $\text{Sm}^{3+}$ -doped  $\text{BaYF}_5$  nGCs and  $\text{Sm}^{3+}$  ions remaining in the silica glassy environment, respectively, indicating that the environment of  $\text{Sm}^{3+}$  ions in the nGCs system is close to an inversion symmetry site. Moreover, by comparing both emission spectra, a blue-shift in the  $\text{Sm}^{3+}$ -doped  $\text{BaYF}_5$  nGCs sample can be observed, which is related to an effect of the different crystal field in both types of environment.

Therefore, all shown results suggest that an important fraction of RE ions is incorporated into the  $\text{BaYF}_5$  NCs in both studied nGCs systems. This is supported by the fact that both ions ( $\text{Eu}^{3+}$  and  $\text{Sm}^{3+}$ ) can occupy the  $\text{Y}^{3+}$  sites with similar ionic radius, without the need for charge compensation, thus increasing the RE solubility. This leads to the conclusion that these nGCs systems are promising candidates as red-emitting phosphors in white LEDs.

## Conclusions

The successful development of sol-gel transparent nGCs, comprising  $\text{Eu}^{3+}$  or  $\text{Sm}^{3+}$ -doped  $\text{BaYF}_5$  NCs, after adequate heat treatments of the corresponding glass

precursors' glasses was achieved. The precipitation into a SiO<sub>2</sub> matrix of BaYF<sub>5</sub> NCs with an estimated size of 11 nm was confirmed by XRD and TEM images. In order to further confirm the presence of cubic BaYF<sub>5</sub> NCs in the nGC system, Eu<sup>3+</sup>-doped BaYF<sub>5</sub> NCs were prepared by solvothermal method and their luminescent properties were studied and compared with the Eu<sup>3+</sup>-doped nGCs. Moreover, the use of Eu<sup>3+</sup> and Sm<sup>3+</sup> as probe ions in the nGCs led us to distinguish between amorphous and like-crystalline environments and confirm the incorporation of a large fraction of RE ions into the BaYF<sub>5</sub> NCs. These results suggest that BaYF<sub>5</sub> nGCs doped with Eu<sup>3+</sup> or Sm<sup>3+</sup> can be considered as potential red-emitting phosphors for the development of white LEDs under near UV excitation.

### **Acknowledgements**

The authors are grateful for financial support to Fundación CajaCanarias (NAFOWLEDs) and IWT (Flemish agency for Innovation by Science and Technology) through the SBO-project LumiCoR (IWT 130030). J. del-Castillo would like to thank Ghent University for his mobility grant and, in particular, the hospitality of LumiLab members during his stay in Ghent.

## References

- [1] W. Niu, S. Wu, S. Zhang, L. Li, *Chem. Commun.* 46, 3908 (2010).
- [2] M. Wang, C. C. Mi, W. X. Wang, C. H. Liu, Y. F. Wu, Z. R. Xu, C. B. Mao, S. K. Xu. *ACS Nano*, 3, 1580 (2009).
- [3] D.Q. Chen, Y.S. Wang, F. Bao, Y.L. Yu, *J. Appl. Phys.* 101 113511(2007)
- [4] K. Zheng, D. Zhao, D. Zhang, N. Liu, F. Shi, W. Qin. *J. Alloys and Comp.* 509, 5848 (2011).
- [5] C. E. Secu, M. Secu, C. Guica, L. Mihut. *Opt. Mater.* 33, 1770 (2011).
- [6] F. Xin, S. Zhao, G. Jia, L. Huang, D. Deng, H. Wang, S. Xu. *Mat. Chem and Phys.* 137, 177 (2012).
- [7] J. del-Castillo, A.C. Yanes, A. Santana-Alonso, J. Méndez-Ramos, *Opt. Mater.* 37 511, (2014).
- [8] J.J. Velázquez, V.D. Rodríguez, A.C. Yanes, J. del Castillo, J. Méndez-Ramos, *Appl. Phys B*, 108, 577 (2012).
- [9] A. Santana-Alonso, A.C. Yanes, J. Méndez-Ramos, J. del-Castillo, V.D. Rodríguez, *Opt. Mater.* 33, 587 (2011).
- [10] J. del-Castillo, A. C. Yanes, J. Méndez-Ramos, V. K. Tikhomirov, V. V. Moshchalkov, V. D. Rodríguez, *J. Sol-Gel Sci. Technol.* 53, 509, (2010).
- [11] T. Grzyb, M. Runowski, S. Lis, *J. Lumin* 154, 479 (2014).
- [12] J. Lin, J. Huo, Y. Cai, Q. Wang. *J. Lumin* 144, 1 (2013).
- [13] X. Changfu, M. Mo, Z. Songjun, R. Guozhong, Y. Liwen, Y. Qibin. *J. Alloys and Compds.* 509, 7943 (2011).
- [14] G. Lunjun, M. Mo, X. Changfu, L. Xujun, W. Suiping, L. Jianguo, Y. Qibin. *J. Lumin* 134, 718 (2013).
- [15] X. S. Quiao, X. P. Fan, M.Q. Wang. *App. Phys. Lett.* 89, 111919 (2006)
- [16] Y. Huang, H. You, G. Jia, Y. Song, Y. Zheng, M. Yang, K. Liu, N. Guo, *J. Phys. Chem. C* 114, 18051(2010).
- [17] Y. Lei, M. Pang, W. Fan, J. Feng, S. Song, S. Danga. H. Zhang, *Dalton Trans.* 40, 142 (2011).
- [18] H. Qiu, G. Chen, L. Sun, S. Hao, G. Han, C. Yang. *J. Mater. Chem* 21, 17202 (2011).
- [19] F. Vetrone, V. Mahalingam, J. A. Capobianco. *Chem. Mater.* 21, 1847 (2009).
- [20] K. Biswas, A. D. Sontakke, K. Annapurna. *Int Journal of App. Glass Science* 3 (2), 154 (2012).

- [21] S. Huang, Q. Gao, M. Gu. *J. Lumin* 132 (3), 750 (2012)
- [22] M. Gu, Q. C. Gao, S.M. Huang, X. L. Liu, B. Liu, C. Ni. *J. Lumin* 132 (10), 2531 (2012)
- [23] F. Liu, Y. Wang, D. Chen, Y. Yu, E. Ma, L. Zhou, P. Huang. *Mat. Lett.* 61, 5022 (2007).
- [24] X.S. Qiao, X.P. Fan, M.Q. Wang, H. Yang, et al., *J. Appl. Phys.* 104, 043508 (2008)
- [25] C. J. Brinker, G. W. Scherer, *Sol-gel science: the physics and chemistry of sol-gel processing* (Academic Press, Boston, 1990)
- [26] P. F. Smet, A. B. Parmentier, D. Poelman. *J. of the Electrochemical Soc.* (6) 158, R37 (2011).
- [27] M. Mo, Y. Liwen, R. Guozhong, X. Changfu, L. Jianguo, Y. Qibin. *J. Lumin.* 131, 1482 (2011).
- [28] S. Cotton, Wiley, West Sussex, UK, Ch. 2, p. 14 (2006).
- [29] A. Biswas, G. S. Maciel, C. S. Friend and P. N. Prasad, *J. Non-Cryst. Solids* 316, 393 (2003).
- [30] S. Fujihara, S. Koji, T. Kimura, *J. Mat. Chem.* 14 (8), 1331 (2004).
- [31] A. C. Yanes, A. Santana-Alonso, J. Méndez-Ramos, J. del-Castillo and V. D. Rodríguez, *Adv. Funct. Mater.* 21, 3136 (2011).
- [32] A.C. Yanes, J.J. Velázquez, J. del-Castillo, J. Méndez-Ramos, V. D. Rodríguez. *Nanotechnol.* 19, 295707 (2008).

## Figure captions

**Fig. 1.** (a) XRD patterns of  $\text{Eu}^{3+}$  doped- $\text{BaYF}_5$  nGCs and  $\text{Eu}^{3+}$  doped- $\text{BaYF}_5$  NCs. Standard peaks of  $\text{BaCeF}_5$  (JCPDS 43-0394) are included for comparison. (b) TEM image of the  $\text{Eu}^{3+}$  doped- $\text{BaYF}_5$  nGCs heat treated at 750 °C.

**Fig. 2.** (a) EDX spectrum of  $\text{Eu}^{3+}$  doped- $\text{BaYF}_5$  NCs. (b) Corresponding HRTEM image. Insets show power spectrum (FFT pattern) and filtered higher-contrasted image of red and blue squared nanoparticles.

**Fig. 3.** Excitation (a) and emission (b) spectra of  $\text{Eu}^{3+}$  doped- $\text{BaYF}_5$  nGCs detecting and exciting at indicated wavelengths. Corresponding excitation (c) and emission (d) spectra of  $\text{Eu}^{3+}$  doped- $\text{BaYF}_5$  NCs, detecting and exciting at indicated wavelengths.

**Fig. 4.** Time-resolved photoluminescence measurements of a  $\text{Eu}^{3+}$  doped- $\text{BaYF}_5$  nGCs exciting at 394 nm and monitoring at 590 nm ( $\text{BaYF}_5$  nGCs nanocrystalline environment) and exciting at 464 nm and monitoring the 616 nm ( $\text{BaYF}_5$  nGCs glassy environment). Inset shows time-resolved photoluminescence measurements of  $\text{Eu}^{3+}$  doped- $\text{BaYF}_5$  NCs exciting at 394 nm and monitoring at 590 nm.

**Fig. 5** Excitation (a) and emission (b) spectra of  $\text{Sm}^{3+}$  doped- $\text{BaYF}_5$  nGCs detecting and exciting at indicated wavelengths. Emission spectrum of  $\text{Sm}^{3+}$  ions in silica glassy environment has also been included for comparison [32].

## Table captions

**Table. 1.** Effective lifetime values of  $\text{Eu}^{3+}$  doped- $\text{BaYF}_5$  nGCs and  $\text{Eu}^{3+}$  doped- $\text{BaYF}_5$  NCs.

Journal of Alloys and Compounds:” **Site selective spectroscopy in BaYF<sub>5</sub>:RE<sup>3+</sup> (RE = Eu, Sm) nano-glass-ceramics”**

- We obtained sol-gel transparent nGCs with Eu<sup>3+</sup>, Sm<sup>3+</sup>-doped cubic BaYF<sub>5</sub> nanocrystals
- Eu<sup>3+</sup>-doped BaYF<sub>5</sub> NCs were prepared by solvothermal method.
- Their luminescent properties were studied and compared with the Eu<sup>3+</sup>-doped nGCs.
- Eu<sup>3+</sup>/Sm<sup>3+</sup> were used as probe ions in the nGCs to distinguish different environments
- The incorporation of a large fraction of RE ions into the BaYF<sub>5</sub> NCs was confirmed.

	$\tau_{\text{eff}}$ (ms)
BaYF <sub>5</sub> nGCs Exc 394 nm Det 590 nm	$9.88 \pm 0.19$
BaYF <sub>5</sub> nGCs Exc 464 nm Det 613 nm	$1.63 \pm 0.03$
BaYF <sub>5</sub> NCs Exc 394 nm Det 590 nm	$9.12 \pm 0.14$

Table. 1.

Figure1

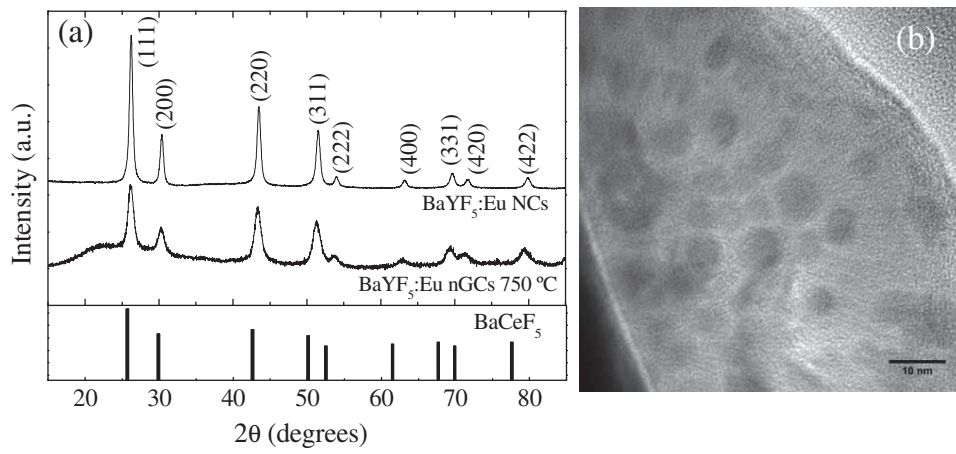


Fig. 1.

Figure2

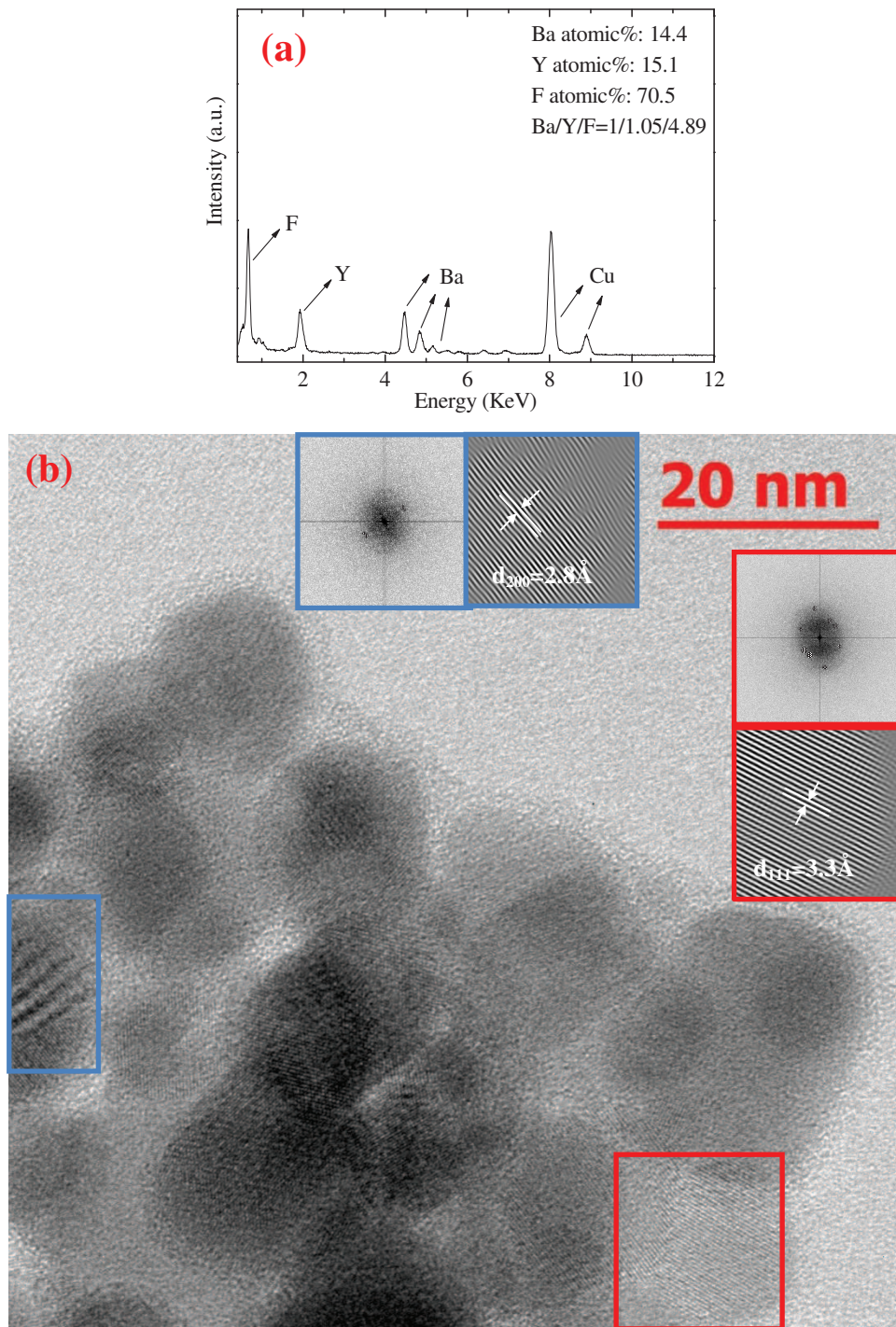


Fig. 2

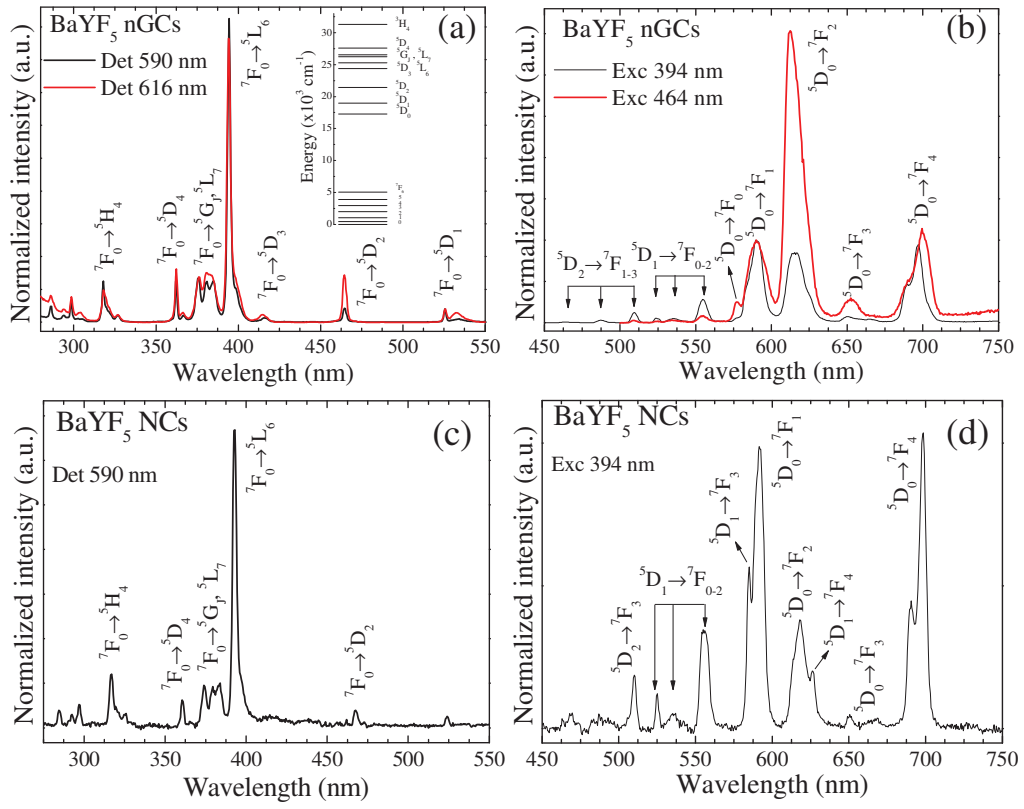


Fig. 3

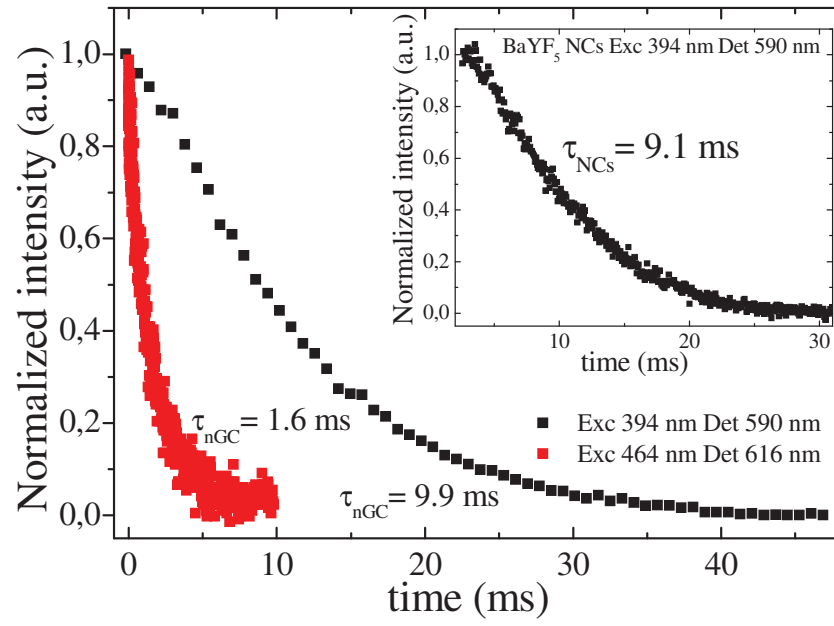


Fig. 4

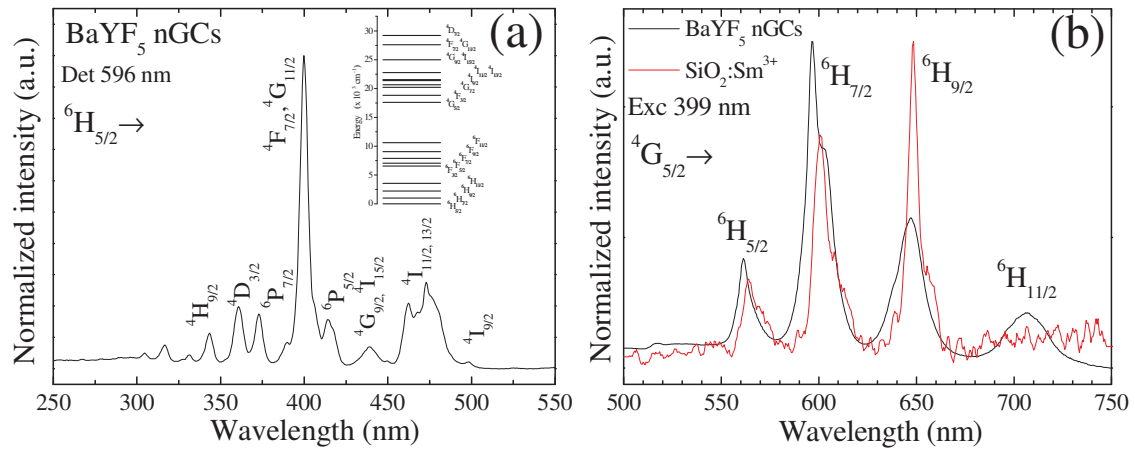


Fig. 5.